Reference: *Biol. Bull.* **187**: 164–173. (October, 1994)

A Model of Rowing Propulsion and the Ontogeny of Locomotion in *Artemia* Larvae

TERRI A. WILLIAMS*

Department of Zoology NJ-15, University of Washington, Seattle, Washington 98195

Abstract. Newly hatched *Artemia* larvae use one pair of limbs to locomote. During development they gradually add additional limbs along the elongating trunk. As larvae grow, body length increases from about 0.4 mm to 4 mm, mean swimming speed increases from 1.8 mm s^{-1} to 9.9 mm s^{-1}, and frequency of antennal beat decreases from 9.5 to 6.7 Hz.

As new limbs are added, they become active in the metachronal rhythm of pre-existing limbs.

The body velocity oscillates as early larvae swim; later larvae swim without a cyclic acceleration and deceleration of the body. The change in the pattern of swimming is correlated with the addition of propulsors and a transition in the relative importance of viscous and inertial effects that determine the propulsion in subsequent stages. Reynolds number (based on body length) increases from 2 to 37.

A theoretical analysis of rowing propulsion at these intermediate Reynolds numbers shows that initial development of new limbs in *Artemia* larvae is unimportant for propulsion.

Rowing propulsion at the low Reynolds numbers is drag-based; as Reynolds number increases, inertial effects become more important, and unsteady forces on the body become significant in the balance between limb and body. A glide of the body develops at the end of the powerstroke, and relative limb velocity changes.

Introduction

Many animals span a broad range of sizes during the course of their complete life cycles. Animals that are active and motile during growth are subject to potentially large differences in the forces they experience during locomotion. Most studies of locomotion have focused on adults whose wings or fins are unlikely to undergo further changes in size or shape (*e.g.*, Wu *et al.*, 1974). Only rarely have comparisons included successive ontogenetic stages of a single species (*e.g.*, Katz and Gosline, 1992). I have analyzed swimming during the larval period in the crustacean *Artemia*. How does function develop in species with active larval forms having different morphologies and locomotory systems than the adults they will become? For animals that swim, ontogenetic changes in size and shape will influence the actual mechanisms by which they propel themselves. Viscous effects predominate in the swimming of very small organisms; inertial effects predominate in the swimming of very large organisms.

The developmental pattern of *Artemia* is unlike that in the more familiar arthropods that exhibit radical changes in body form from one molt to the next. These small crustaceans change gradually as they grow; *i.e.*, they are anamorphic developers. When they hatch, they swim with one pair of limbs, the second antennae (hereafter antennae). These limbs dominate propulsion during the first half of larval life and are gradually succeeded by a series of limbs that develop sequentially on the trunk. In contrast to an animal that radically changes its morphology between one molt and the next, an *Artemia* larva must coordinate new pairs of limbs with pre-existing ones (Fryer, 1983). The antennae and the trunk limbs are coordinated in a metachronal rhythm, while growth and the gradual acquisition of new limbs effectively reset the body trajectory and the relative motions of the limbs and body at each stage. How does locomotion change as an animal proceeds through the size and shape changes of ontogeny?

To explore changes in the mechanics of swimming in animals too small for direct measurement, I built a physical model of the limb to empirically determine force coefficients acting in flow regimes relevant to developing *Ar-*

Received 4 June 1993; accepted 19 July 1994.

* Present address: Department of Anatomy, University of Vienna, Währingerstrasse 13, A-1090 Wien, Austria.

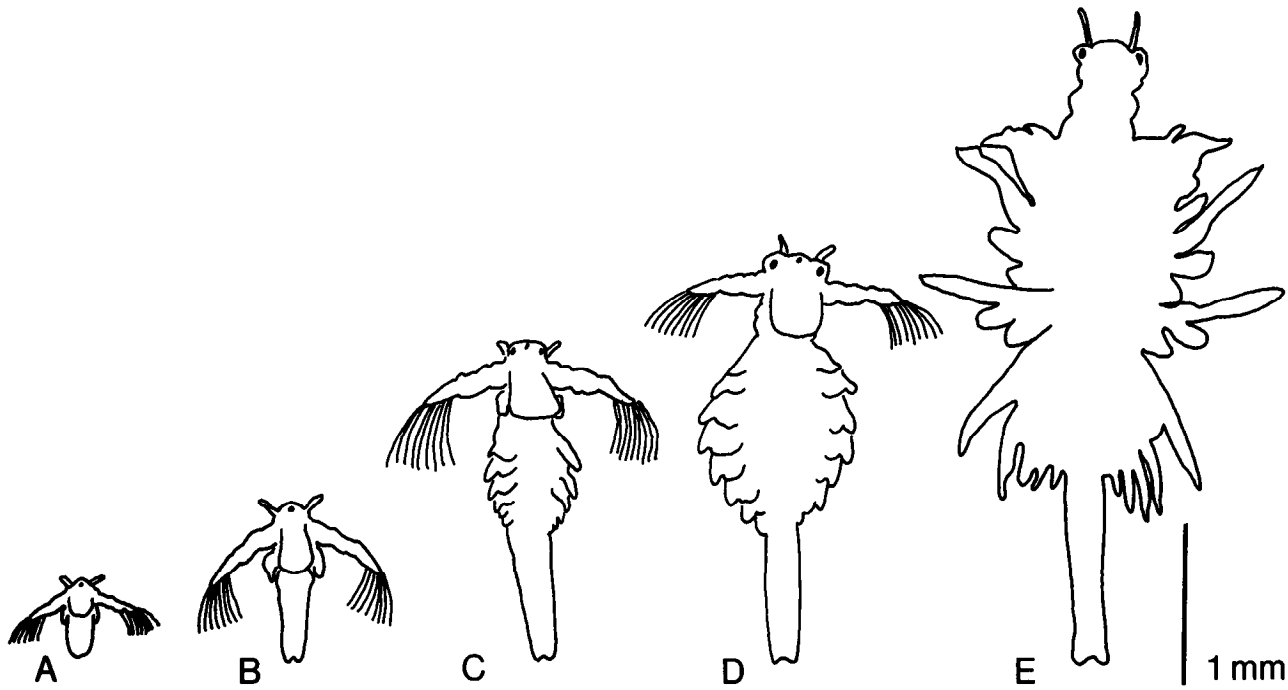

Figure 1. Selected stages to show the gradual development of *Artemia* larvae. (A) Nauplius. (B) Post-nauplius with rudiments of limbs developing on the trunk. (C) Larva with four active trunk limbs. (D) Larva with eight active trunk limbs. (E) Animal with 11 active trunk limbs.

temia larvae (Williams, 1994). Here I develop a theoretical model of swimming by antennal propulsion that incorporates those results. I predict the swimming movements of a body propelled only with a single pair of limbs by balancing the thrust produced by the limbs with forces on the body that resist motion. Because the larvae use only one pair of limbs upon hatching, I can compare body movements predicted by the model with actual movements of the larvae and thus evaluate the accuracy of the model. I then ignore the development of trunk limbs and ask, How would swimming change if the initial propulsive system were scaled up in exactly the same way the larvae grow? How would the antennae alone drive the body at later larval stages? Comparisons with actual later stage larvae allow me to dissect increases in size from changes in morphology. Does functional change correlate simply with morphological change? *e.g.*, how important are the additional trunk limbs in generating thrust?

Past studies of locomotion have been based on the assumption that thrust production by small rowing animals is purely drag-based (Nachtigall, 1980; Zaret and Kerfoot, 1980). Although *Artemia* hatchlings swim at fairly low Reynolds numbers, they grow through a size and speed range that includes fluid regimes in which inertia becomes important. Not only does drag scale differently at low and high Reynolds numbers, but also, at high Reynolds numbers, momentum can be transferred simply by the accelerations and decelerations of fluids (Daniel, 1984). I include both of these possible scale effects such that the model is free to reflect the different flow regimes that the larvae experience.

Materials and Methods

Animals

Artemia larvae grew at room temperature (~ 21°C) in an aerated brine solution of 35–40‰; the animals fed on varying diets of yeast and green algae. The number of molts was not crucial to my study, so I staged the larvae as follows: (1) newly hatched larva (nauplius)—the most oblate form with no differentiation of the trunk region, yolk still present; (2) larvae with visible limb buds—differentiation in the trunk region has led to visible protrusions of what will be limbs, and body is more elongate; (3) a series of larval stages identified by the number of actively beating trunk appendages present. This series of stages terminated with forms that have attained the adult complement of 11 pairs of trunk appendages and have lost the larval form of the second antennae (Fig. 1).

Filming

I filmed the larvae with a Locam high-speed movie camera running at 200 frames per second. The time between frames, 0.005 s., was accurate to ~5% as measured by the slippage of a timing marker made by the camera

on the edge of the film. Either an Olympus BH microscope with transmitted illumination or a Wild M5 dissecting scope with fiber optic epi-illumination magnified the animals for filming. I tried to minimize wall effects by designing the filming chambers according to the formula, $y/\ell > 20/Re$, to calculate y, the shortest distance to the nearest wall (Vogel, 1981), where ℓ is some characteristic length. I chose body length. I used chambers: 22 × 22 × 5 mm and 22 × 22 × 8 mm. The animals tended to swim in a plane parallel to the bottom of the chamber and, therefore, to stay roughly in mid-chamber. However, since the animals were free-swimming, the actual sequences captured on film and digitized came from various locations within the chamber.

The obvious constraints of using high-speed cine-photography to film free-swimming animals prevented me from gathering data on many individuals from each stage. Results here are from measurements on individuals and reflect the clearest and most complete sequences. The results are limited because I cannot include variation, either individual or stage-specific, but they are supplemented by hours of viewing time that confirm the developmental trends I present. My description is supported by Barlow and Sleigh (1980), who report limb beat frequencies of 8–10 Hz in early stages and 6–7 Hz in later stages, and the same increase in both absolute and relative body length. Larvae do show variation in limb length, etc., at a given stage—due in part to rearing conditions—but this variation should not materially change the gross developmental trends reported here.

I digitized body motions from the films with a Bitpad digitizer. I chose sequences in which the animal remained in the plane of focus and digitized both the anterior- and posterior-most point on the body. The variability in measurements of body length ranged from a standard deviation of 0.01 mm in the smallest animal, to 0.05 mm in the largest. The distance between the two points provided a measure of body length, and the displacement of a single point in successive frames provided a measure of body velocity.

I quantified limb motions by digitizing the most proximal and distal points along the limb plus an arbitrary number of points along the edge of the limb. The collection of points from each frame defined a curve that could subsequently be fit with a small number of segments to calculate relative velocities along the limb. This procedure precluded the problem of trying to follow ill-defined landmarks on the limb from one frame to the next.

To quantify the asymmetry of stroke due to the curling of the antennae and the collapse of setae during the recovery stroke, I measured the projected area, S_a, of the limb perpendicular to the body axis at the 90° position during the power stroke and the recovery stroke and computed the ratio of the two areas.

Force balance for predicted body velocity

To predict the instantaneous motion of a body propelled by a single pair of limbs, I used a simple linear momentum balance (*e.g.*, Daniel and Webb, 1987) for the forces of the limbs and forces on the body.

I prescribe the variation of limb angle with respect to the long axis of the body, or angular position, θ, based on sinusoidal motion:

$$\theta(t) = \theta_o + (A/2)\,(1 - \cos(\omega t)); \quad (1)$$

where A is the amplitude of limb beat and ω, the angular frequency, $= 2\pi f$, (f = frequency), and θ_o is the starting angle (Fig. 2).

Limb speed at the tip of the limb is given by a linear combination of its angular frequency and the speed of the body (U_b). I assume flows parallel to the limb contribute negligibly to thrust. The normal component of limb velocity, U_a, is given by:

$$U_a = (-\ell d\theta/dt + U_b \sin\theta); \quad (2)$$

where ℓ = length of the antenna and U_a depends on $-(\ell d\theta/dt)$ due to the convention of choosing forward body velocity as the positive direction (*i.e.*, thrust acts in the opposite direction).

I use this speed to calculate two types of forces that might arise from limb motion: the drag force and the unsteady, or added mass, force. I assume that the limb moves symmetrically about the axis perpendicular to the body and that only the component of flows parallel to the long axis of the body contribute to generating thrust.

The drag force of the limb, D_a, is proportional to the velocity normal to the limb and is perpendicular to the limb in direction:

$$D_a = 0.5\rho S_a (U_a)^2 C_{da}; \quad (3)$$

where ρ is the density of the fluid, S_a is the projected surface area of the limb, and C_{da} is the coefficient of drag on the limb. The ratio of surface area on the power stroke to recovery stroke is 3.3:1.

For both C_{da} and C_{db}, the coefficient of drag on the body, I use $C_d = 1 + 10Re^{-2/3}$. I use this coefficient of

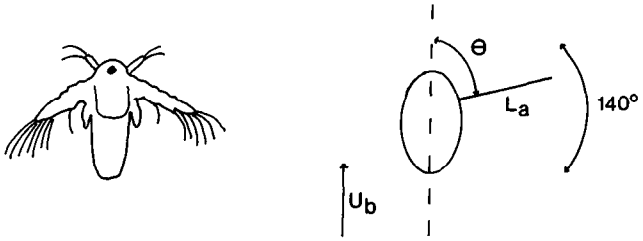

Figure 2. Forces on a pair of limbs are calculated on the basis of a prescribed sinusoidal motion. These are balanced by forces acting on a body to give instantaneous body velocity. U_b is body velocity, L_a is limb length, and θ is limb angle relative to the long axis of the body.

Table I

Morphological and kinematic parameters of selected larval stages and comparison to model predictions

	Measured values					Model predictions	
Stage	Body length (mm)	Antennal length (mm)	Freq. (Hz)	Average speed (mm s^{-1})	Reynolds number	Reynolds number (pred.)	Volume/ stroke (normalized)
Nauplius	0.39	0.25	9.5	1.8	2	2	1.2×10^{-2}
Limb bud	0.77	0.5	9.1	4.4	5	9	1.8×10^{-2}
Limb bud	0.77	0.5	9.1	3.3	5	NA	NA
4 trunk limbs	1.79	0.6	8.3	8.4	14	17	4.3×10^{-2}
8 trunk limbs	2.58	0.6	6.7	8.1	20	NA	NA
11 trunk limbs	3.87	*	5.1	9.9	37	NA	NA

NA: Comparison not made.
* Metamorphosed into adult form.

drag because it most accurately mimics the behavior of a physical model of the limb tested under similar hydrodynamic conditions (Williams, 1994). The Reynolds number, $Re = \rho \ell U/\mu$, where ρ = fluid density, ℓ = some characteristic linear dimension of the object—in this case the length of the limb—U = average speed, and μ = viscosity of the fluid. To calculate C_{db}, I divide the expression for C_d at intermediate Reynolds numbers by 1.5 to account for the long axis of the body being parallel to flow instead of perpendicular to flow (Vogel, 1981). In this case, the characteristic length for Reynolds number calculations is body length.

I also account for any unsteady forces that arise in the fluid as a result of the acceleration of the fluid adjacent to the limb. Unsteady forces are proportional to the rate of change of the velocity of the limb; I assume the component parallel to the limb contributes negligibly to thrust. I define the acceleration of the limb:

$$dU_a/dt = (-\ell d^2\theta/dt^2 + dU_b/dt \sin \theta). \quad (4)$$

The unsteady force on the limb, G_a becomes:

$$G_a = \alpha \rho V_a dU_a/dt; \quad (5)$$

where α is the added mass coefficient, which I assume = 1 (Daniel, 1984), and V_a is the volume of the limb, which I assume to be cylindrical.

The sum of the drag and unsteady forces, (3) and (5), gives the total thrust produced by the limb:

$$F_a = 0.5\rho S_a(-\ell d\theta/dt + U_b \sin \theta)^2 C_{da} + \alpha \rho V_a(-\ell d^2\theta/dt^2 + dU_b/dt \sin \theta). \quad (6)$$

This force is balanced by the two analogous forces on the body as well as by body inertia, and the total momentum balance becomes:

$$2[0.5\rho S_a U_a^2 C_{da} + \rho V_a dU_a/dt] = 0.5\rho S_b U_b C_{db} + 2\rho V_b dU_b/dt; \quad (7)$$

where S_b = the surface area of the body and V_b = the volume of the body, which I assume to be a cylinder whose volume is calculated based on body length. Limb forces are multiplied by 2 to account for the pair of limbs.

I solve for U_b numerically using a fourth order Runge-Kutta numerical scheme (Boyce and DiPrima, 1977); I wrote the computer code. For each larval stage simulated by the model, I input frequency of antennal beat (f), body length (ℓ_b), and antennal length (ℓ_a), all measured from high-speed films.

Results

Kinematics

What limbs are present and active as the larvae mature? *Artemia* hatches as a nauplius larva: the body is ovoid and bears three pairs of appendages (Fig. 1) that beat metachronally. But because the other two pairs of limbs are small relative to the antennae, the animal effectively swims with only the antennae. The antennae are approximately 0.3 mm long and project laterally from the body; they are cylindrical in cross-section and covered by a flexible cuticle. The distal part of the limb bifurcates and bears long setae that fan out in a plane perpendicular to the direction of forward swimming. This fan accounts for approximately 75% of the projected surface area of the limb and, as the limb oscillates in a rowing motion, it alternately opens and shuts.

As *Artemia* passes through successive larval stages, the body elongates 10-fold (from 0.39 mm to 4 mm; Table I), and limbs are added serially along the lengthening body (Fig. 1). These limbs gradually overtake the antennae in size. In contrast to the cylindrically shaped antennae that

project laterally, the trunk limbs are flat, leaflike appendages that project ventrally from the body. These limbs grow gradually, with the anterior-most appendages developing first. At any given time there is a series of trunk limbs in progressive stages of maturity; the full development of each limb requires several molts. The antennae remain similar throughout larval development, although their length relative to body length decreases (Table I).

How does the body move at different stages? The average swimming velocity increases during development from roughly 2 mm s^{-1} to 10 mm s^{-1}. This increase in speed coupled with the increase in body length leads to a change in Reynolds number from 2 in the newly hatched larva to almost 40 in the last larval stage (Table I). The time-course of body motion changes even more strikingly. The young nauplius ratchets through the water at high frequency, each beat cycle yielding a discrete forward lurch and backward slip of the body. There is no glide in the nauplius: at the end of the power stroke, the body virtually stops moving (Fig. 3A). The effect is a visibly jerky mode of swimming due to the continuous oscillation of the body back and forth in the water.

Later, as the more complicated rhythms of the developing metachrony of the trunk limbs arise, the axial body movements, although still pulsatile, gradually become less so. As the initial trunk limbs develop, the body develops a glide past the end of the power stroke of the antennae. This glide grows in duration as more limbs develop and begin to beat (Fig. 3B). When four pairs of trunk appendages are beating, the larvae no longer experience any backward motion. The role of the antennae is still quite distinct: as in the earliest stages, the peak body velocity is midway during the power stroke of the antennae (0.03 s; Fig. 3C), indicating that the power stroke still produces the greatest thrust. With eight pairs of trunk limbs present, the body still oscillates in the water, but multiple limbs act simultaneously to propel the animal, so it is difficult to relate the movement of the body to the action of any single pair of limbs (Fig. 3D). After 11 pairs of trunk appendages are added, the larval form of the antenna is lost. The movement of the body at this stage is more or less smooth and nonoscillatory (Fig. 3E).

The movement of the limbs relative to surrounding fluid changes. The stereotyped stroke of the antennae relative to the body during larval development does not result in a stereotyped pattern of movement relative to the surrounding fluid. Figure 4 shows the velocity distribution relative to still water along the length of the antennae for two stages: a newly hatched larva and a larva with four actively beating trunk limbs. For a newly hatched larva, midway through the power stroke (first half of the graph, Fig. 4A), the velocity near the distal end of the appendage is actually lower than at the proximal end. This velocity distribution along the limb makes it appear as though the limb virtually pivots around a point near the distal part of the limb. In later stages, the distal portion of the antennae moves faster than the more proximal parts (Fig. 4B).

Model predictions

Comparison of larval body trajectories and predicted body trajectories. Although the model is based on thrust production by a single pair of limbs, it predicts some of the changes in body trajectory experienced by the morphologically complex larvae. Figure 5 shows the measured body velocity per limb beat cycle superimposed on body velocities predicted by the mathematical model for an animal similar to each stage in body and antennal lengths and limb beat frequency (Table I). The predicted body velocities mimic measured larval body velocities in certain important respects:

1. The model predicts a negative body velocity during the recovery stroke; this is large for early stages and decreases in later stages. The decrease in the degree of axial oscillations in swimming (*i.e.*, positive and negative body velocities associated with the power and recovery strokes) predicted by the model closely matches the movement of a larva with no active trunk limbs (Figs. 5A, B) and even that of a larva with four active trunk limbs (Fig. 5C). At the stage where eight trunk limbs are continuously and metachronally active, the animal swims more smoothly than the model—which is based on antennal rowing alone—predicts (Fig. 5D).
2. The negative velocity of the body, associated with the recovery stroke of the antennae, is delayed in successive larval stages. The model predicts this delay: in small animals the body slips backward with the onset of the recovery stroke halfway through the limb beat cycle; in larger animals a glide develops that carries the body forward beyond the onset of the recovery stroke.
3. During early larval stages, the magnitude of body velocity increases. The model also reproduces this trend (Fig. 5A–C).

Balance of forces. Figures 6A–C represent the balance of forces through the single cycle of limb motion that produced the predicted swimming trajectories in Figures 5A, B, C. The most striking change during development is the increase in the contribution of the unsteady forces on the body. Initially, the Reynolds number is low, ~2 (Table I), and the interaction of limb and body viscous drag forces largely determines the body velocity. In later stages, unsteady effects come into play. Unsteady forces on the body tend to resist changes in body velocity. At the onset of the power stroke, they resist acceleration of the body. These trends make the limb and body motions

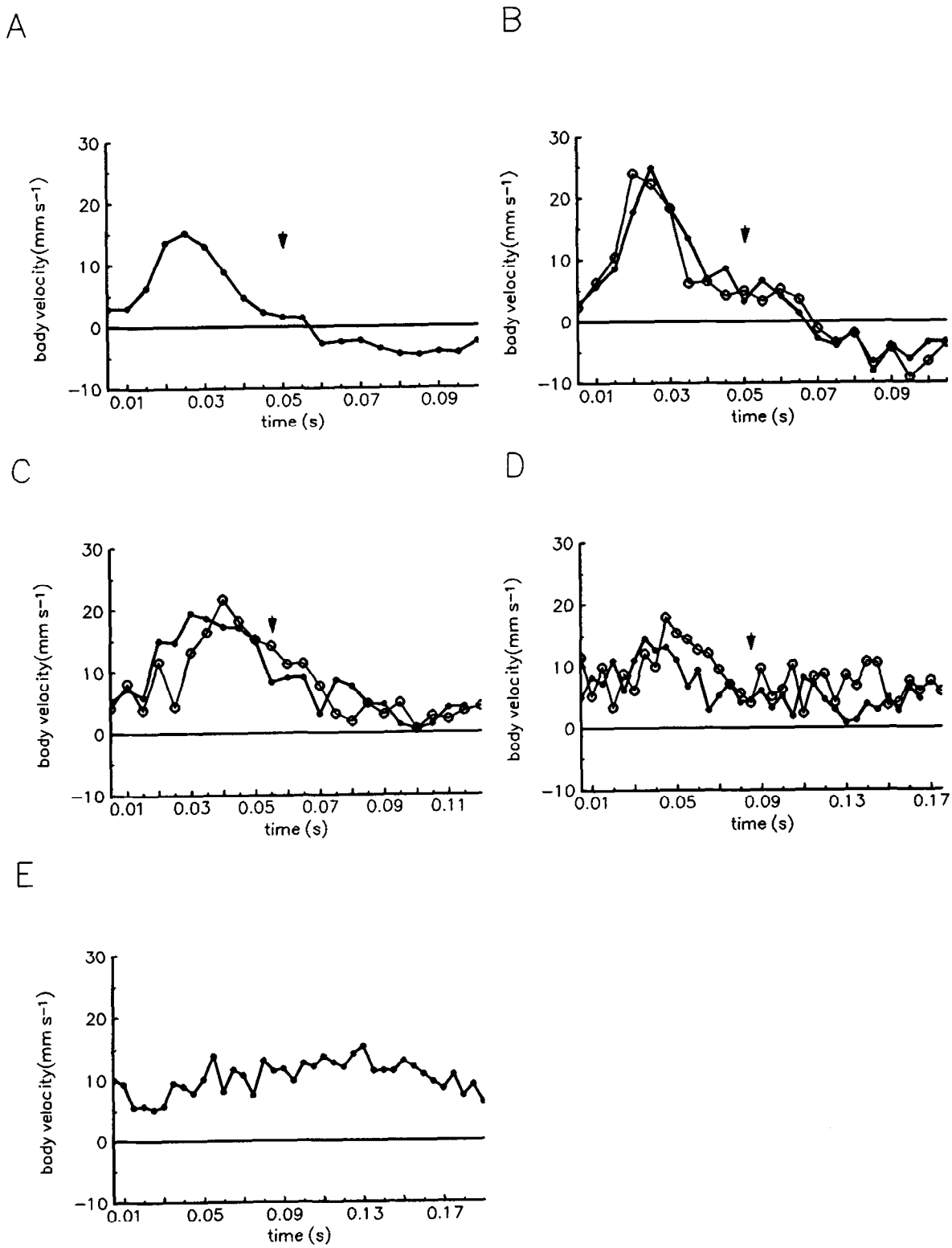

Figure 3. Body velocity of *Artemia* larvae (relative to still fluid) at different stages in larval development. Letters designate stages as indicated in Figure 1. Negative velocity represents backward movement of the body in the water. Arrows mark onset of recovery stroke. B–D illustrate two individuals each to give an idea of individual variation.

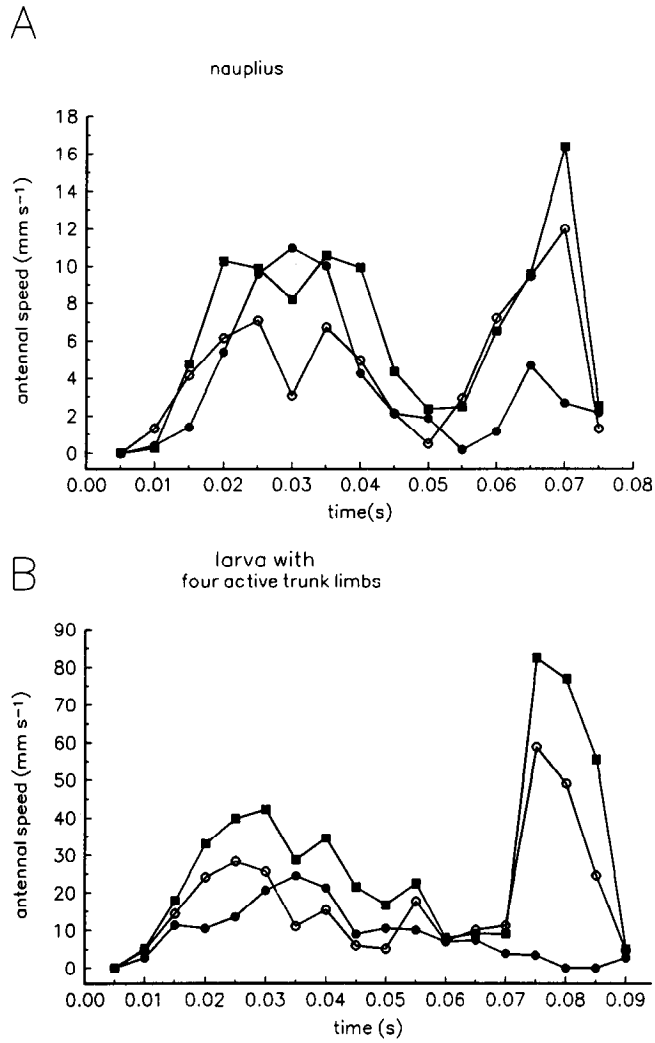

Figure 4. Typical velocity distribution of three points, from proximal to distal, along the antennae for a representative nauplius (A) and a larva with four active trunk limbs (B). Proximal point, filled circles; mid-point, open circles; distal point, filled squares. Both graphs begin at the onset of the power stroke and measure velocity relative to a fixed frame of reference.

out of phase; peak limb velocity precedes body velocity as thrust is required to overcome the unsteady forces on the body (Fig. 7). At the end of the power stroke, however, when the limb undergoes reversal, unsteady forces on the body resist deceleration and tend to carry the body forward even as the limb is generating negative thrust (Fig 6B). These unsteady forces increase in simulations of later stages, giving rise to an increased glide on the body (Fig 6C).

How do the propulsive limbs operate differently as the balance of forces changes? The change in the balance of forces during growth gives rise, not only to differences in body velocity during a cycle of limb beat, but also to differences in the movement of the propulsive limbs. As stated above, the growth of unsteady effects shifts the phases of peak limb motion relative to peak body motion. In addition, the velocity distribution along the limb, relative to still water, changes with the growth of unsteady effects. When limb and body movements are in phase, the distal part of the limb moves relatively little with respect to distant surrounding fluid as it swings in the power stroke (Fig. 7A). In contrast, with the shift in phase predicted for later stages, the limb sweeps a broad arc through the water. This change mimics the one in relative antennal velocity measured from high-speed films (Fig. 4A, B). To index the change in relative antennal velocity, I calculated the volume of space through which the distal one-third of the limb moves. To allow comparison between different stages, I normalized these volumes by dividing by the length of the limb cubed. In simulations of later stages, the limbs move through a proportionately greater volume than in earlier stages (Table I).

Discussion

Artemia develop from a small, rotund nauplius that ratchets along with one pair of oars to a multi-limbed adult that glides continuously through the water. As the animals approach the adult morphology by growing and adding limbs along the trunk, their average swimming speed increases and, more strikingly, the jerky swimming of the hatchling is transformed into the smooth gliding of the adult. The gradual change in swimming corresponds to the gradual addition of trunk limbs. But, as indicated by the increase in Reynolds number during development, this change in swimming also corresponds with a change in forces that determine movement. When *Artemia* hatch, viscous forces have a large role in the flows around the animal: abrupt reversals of the limb are manifest immediately as abrupt changes in body motions. As larvae grow, inertial effects become more important: the body is carried beyond the immediate movement of the limbs. A theoretical analysis of rowing locomotion shows that early changes in kinematics are purely a mechanical consequence of scaling and not tightly linked to the complex morphological changes the larvae undergo. The activity and coordination of trunk limbs appear unimportant for propulsion during early stages, even when four trunk limbs are actively beating.

This result depends on the fact that as inertial forces play an ever greater role in propulsion, unsteady forces on the body begin to develop. Unsteady effects are predicted to provide thrust for animals with oscillating limbs (Daniel, 1984). From kinematic analysis of successive stages of larval herring, Batty (1984) postulated that the change in undulatory swimming in later larval stages is due to increasing importance of inertial effects. Blake (1986) calculated that unsteady forces on the limbs of

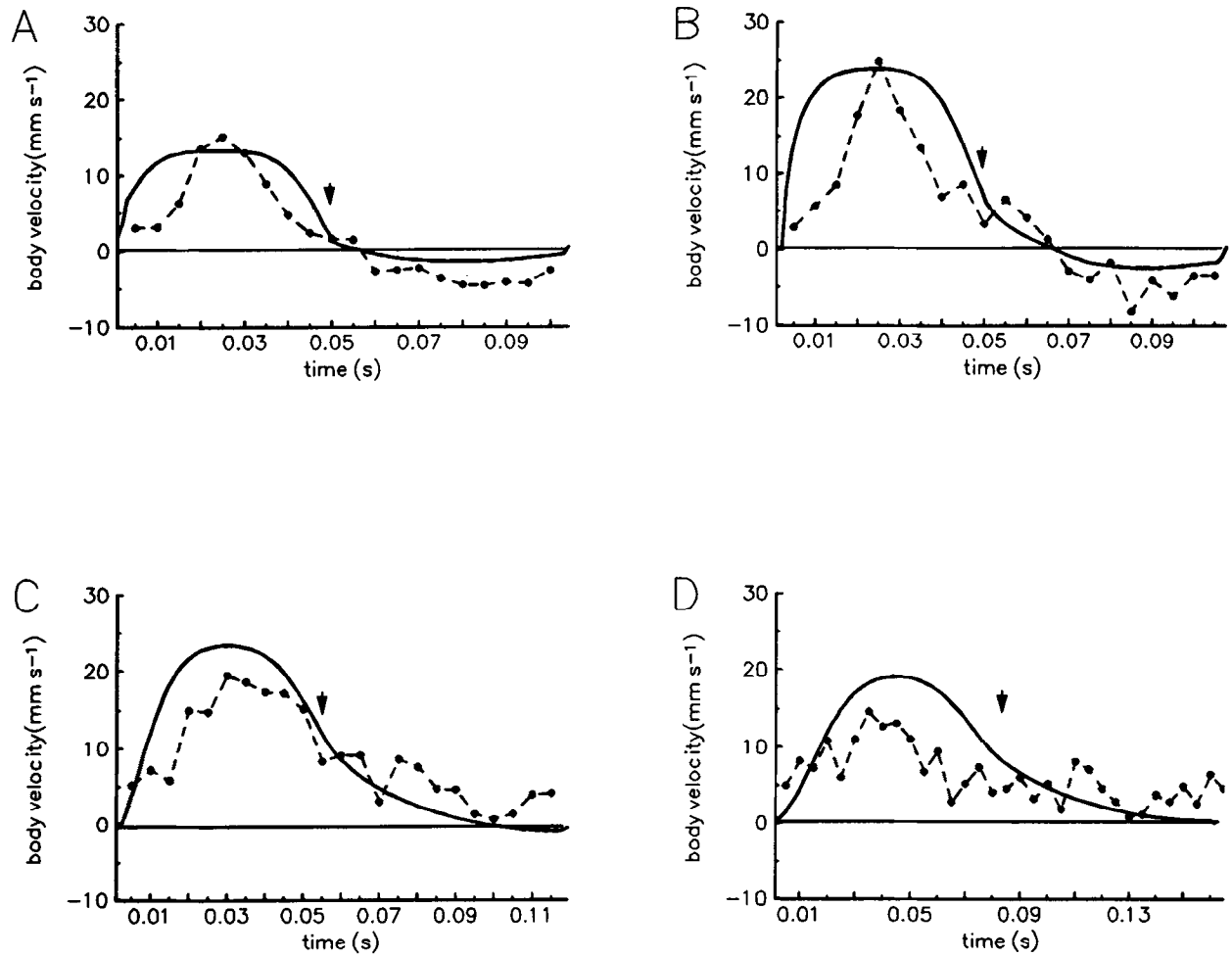

Figure 5. Measured body trajectory of *Artemia* larvae that are both growing and adding limbs, compared with the predicted velocity of an animal with a single pair of limbs but of the same dimensions and frequency as the developing larvae (see Table I). The solid lines illustrate body motion through one cycle of antennal motion for four different larval stages corresponding to A–D in Figure 3. The dotted lines represent body motion predicted by the model. Negative velocity indicates backward movement of the body relative to the fluid. Arrows mark onset of recovery stroke.

rowing water boatmen (Re = 800) could produce roughly one-third of the thrust during the power stroke. As a result of increases in larval size and speed, unsteady effects on the body grow and cause the balance between limb and body to shift. This shift results in a glide of the body at the end of the power stroke and a higher relative velocity at the tip of the limb. Unsteady forces calculated for the limb are negligible, a result corroborated by force measurements on a physical model of an antenna operating at similar Reynolds numbers (Williams, 1994).

Mechanical analyses of animals that paddle have typically dealt only with the adult form and have assumed forward, steady motion (*e.g.*, Blake, 1979; Nachtigall, 1980). Because it does not assume steady motion, but instead couples limb and body motion, the model is free to predict changes in the *time course* of swimming motion on the basis of changes in hydrodynamic regime. Interpretations of biologically relevant flows based on Reynolds numbers calculated from time-averaged swimming speeds may fail to recognize the potential importance of unsteady effects in animals that use reciprocating limbs. In this model, one system of oscillating limbs produces different swimming behaviors even over a narrow range of Reynolds numbers, 2–40.

The antennae that propel the hatchling remain present and grow as the animal grows, and they continue to move in a stereotyped manner. Because of their coupling to the body, they have a different velocity profile along their length as the force balance between limbs and body changes during larval development. This is likely to have consequences for the function of these limbs. Cheer and Koehl (1987) have shown theoretically that structures such

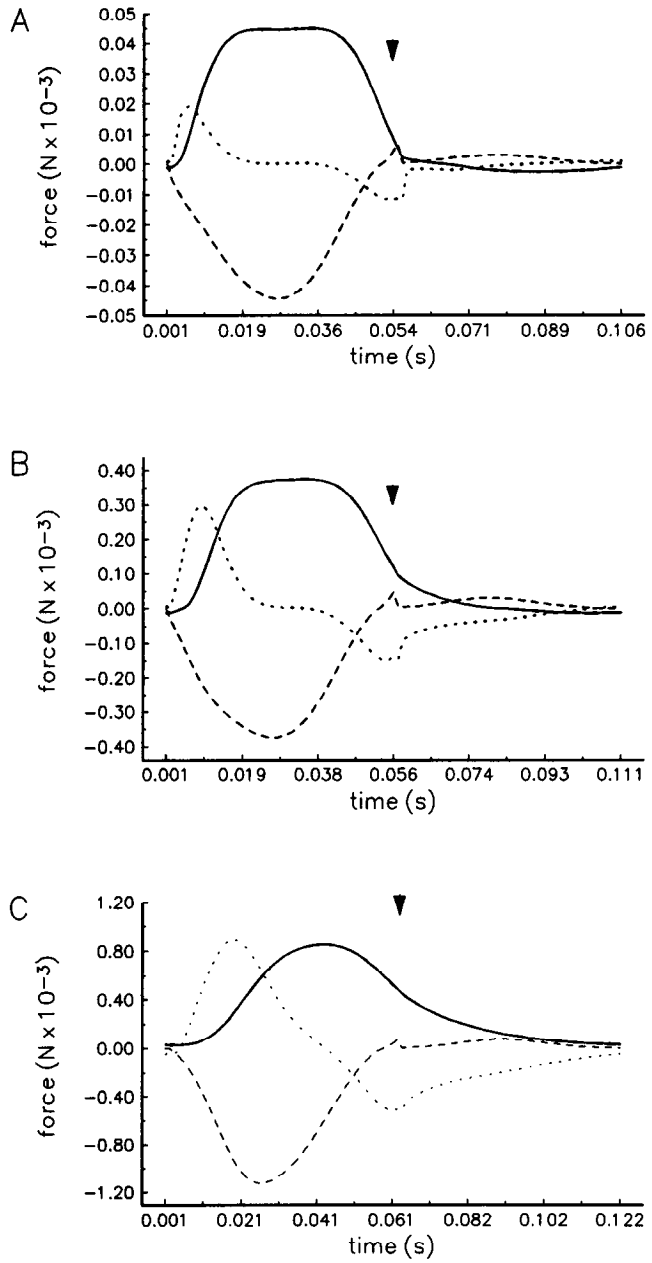

Figure 6. Balance of forces through one cycle of the antennal motion that gives rise to the body motions predicted in Figure 5A–C. By convention, positive thrust is in the direction opposite to forward body motion. Solid line = body drag; dashed line = thrust of limb; dotted line = unsteady force on the body. In C, the unsteady force on the body propels the body beyond the onset of the recovery stroke. (The calculated unsteady force on the limb was always 2 orders of magnitude lower than any other force and is omitted from the graphs.) Arrows mark onset of recovery stroke.

as setose limbs (*i.e.*, cylinders bearing other cylinders), will either allow fluid through the array or force it around, depending on the importance of viscous drag. Some copepods do not use a sweep net to feed, but individually handle fluid parcels surrounding a food item (Koehl, 1981). Other species use the same appendage and the same movements essentially as a filter. In spite of the stereotypic form and movement of the antennae of *Artemia* larvae, their movement relative to the surrounding fluid changes during development. This change in relative limb velocity agrees with a study by Barlow and Sleigh (1980), who postulate that early stages may be unable to capture food because of the relatively low fluid velocities at the distal end of their antennae. A similar conclusion is reached by Fryer (1983) for another anostracan, *Branchianecta ferox.*

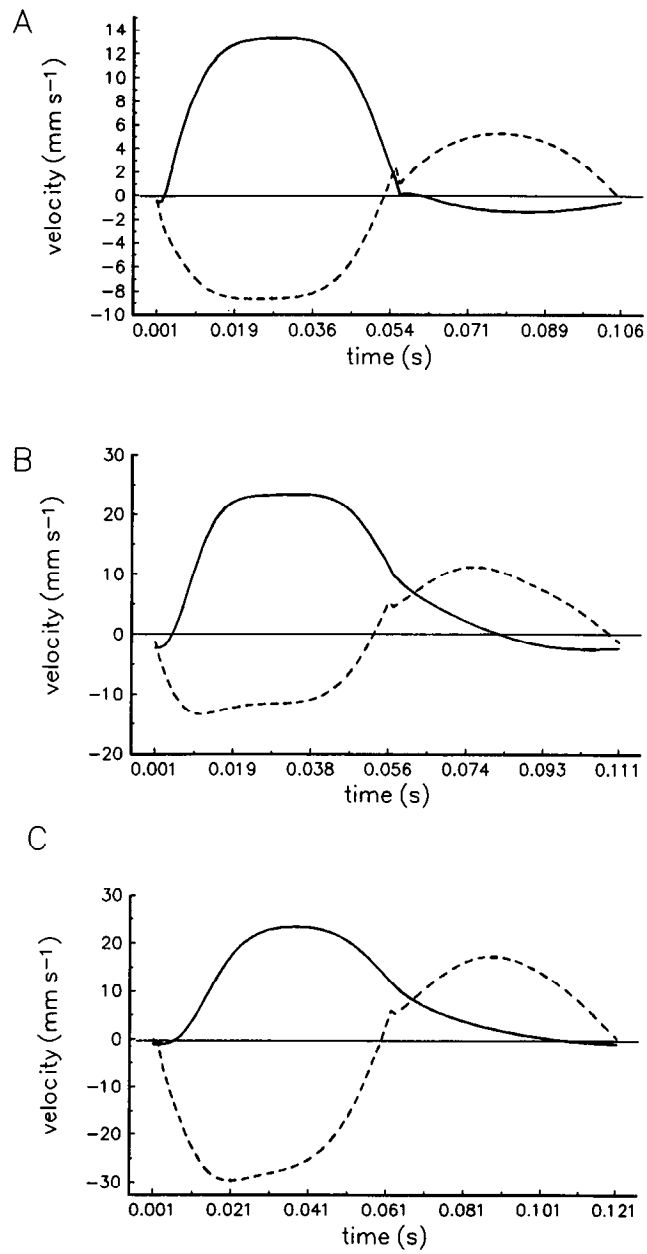

Figure 7. Relative limb and body motions corresponding to Figure 6A–C. Solid lines = body velocity; dotted lines = limb velocity. Positive velocity is in the direction of body motion.

He excludes the possibility that the distal setal fan on the larval antennae functions in feeding and postulates that this function is performed by a spine in a more proximal position on the limb. Levering or stepping through the water generally occurs in larvae that use a single pair of oars. This movement, which occurs in barnacle larvae (pers. obs.), limits our using tethered animals to study behaviors that depend on natural flow situations (*e.g.*, feeding; Moyse, 1984), even though such studies do isolate and help clarify other aspects of movement.

In insects, the aerodynamic and thermodynamic capabilities as measured by physical models scale differently with size: in small models, wings of a particular size function primarily in thermoregulation. In large models of the same relative wing length, the function of the wings is primarily aerodynamic (Kingsolver and Koehl, 1985). That analysis showed that function could simply change with size over the course of evolutionary time. This analysis of swimming in *Artemia* shows that changes in size, shape, and environment experienced by *single* individuals during larval development have consequences for the propulsive mechanisms used in swimming.

Artemia larvae pass through a series of morphological stages as they develop. Functional change may or may not correspond directly to morphological change; *e.g.*, I claim that activity of initial trunk limbs is unimportant in propulsion in *Artemia* larvae, although these limbs obviously propel later stages. Initially, these limbs could perform other roles not treated by this analysis, either mechanical (*e.g.*, stability), or nonmechanical. This model provides a mechanical analysis of swimming on the basis of the morphology of one larval stage in *Artemia*. A single pair of oscillating limbs generates body velocities that mimic the kinematic changes of an early period of development. These results illustrate how, at a particular stage in development, larval morphology engenders a range of behaviors by its very design.

Acknowledgments

I gratefully acknowledge grants from Sigma Xi, the Lerner-Grey fund for Marine Science, NSF grant DCB-8711654 to Tom Daniel, NSF grant BSR-8700523 to Alan Kohn. Tom Daniel, Joel Kingsolver, Alan Kohn, Garry Odell, Dick Strathmann, and Steve Wainwright criticized this paper at various stages.

Literature Cited

Barlow, D. I., and M. A. Sleigh. 1980. The propulsion and use of water currents for swimming and feeding in larval and adult *Artemia*. Pp. 61–73 in *The Brine Shrimp Artemia. Vol 1. Morphology, Genetics, Radiobiology, Toxicology*, G. Persoone, P. Sorgeloos, O. Roels, and E. Jaspers, eds. Universa Press, Wetteren, Belgium.

Batty, R. S. 1984. Development of swimming movements and musculature of larval herring (*Clupea harengus*). *J. Exp. Biol.* **37:** 129–153.

Blake, R. W. 1979. The mechanics of labriform locomotion. I. Labriform locomotion in the anglefish (*Pterophyllum eimekei*); an analysis of the power stroke. *J. Exp. Biol.* **82:** 255–271.

Blake, R. W. 1986. Hydrodynamics of swimming in the water boatman, *Cenocorixa bifida*. *Can. J. Zool.* **64:** 1606–1613.

Boyce, E., and R. C. DiPrima. 1977. *Elementary Differential Equations.* John Wiley and Sons, New York. 512 pp.

Cheer, A. Y. L., and M. A. R. Koehl. 1987. Paddles and rakes: fluid flow through bristled appendages of small organisms. *J. Theor. Biol.* **129:** 17–39.

Daniel, T. L. 1984. Unsteady aspects of aquatic locomotion. *Am. Zool.* **24:** 121–134.

Daniel, T. L., and P. W. Webb. 1987. Physical determinants of locomotion. Pp. 343–369 in *Comparative Physiology: Life in Water and on Land*, P. Dejours, L. Bolis, C. R. Taylor, and E. R. Weibel, eds. Liviana Press, New York.

Fryer, G. 1983. Functional ontogenetic changes in *Branchinecta ferox*. *Phil. Trans R. Soc. Lond. B* **303:** 229–343.

Katz, S. L., and J. M. Gosline. 1992. Ontogenetic scaling and mechanical behavior of the tibia of the african desert locust (*Schistocerca gregaria*). *J. Exp. Biol.* **168:** 125–150.

Kingsolver, J. G., and M. A. R. Koehl. 1985. Aerodynamics, thermoregulation, and the evolution of insect wings: differential scaling and evolutionary change. *Evolution* **39:** 488–504.

Koehl, M. A. R. 1981. Feeding at low Reynolds number by copepods. *Lect. Math. Life Sci.* **14:** 89–117.

Moyse, J. 1984. Some observations on the swimming and feeding of the nauplius larvae of *Lepas pectinata* (Cirripedia: Crustacea). *Zool. J. Linn. Soc.* **80:** 323–336.

Nachtigall, W. 1980. Mechanics of swimming in water beetles. Pp. 107–124 in *Aspects of Animal Movement*, H. Y. Elder and E. R. Trueman, eds. Cambridge University Press, London.

Vogel, S. 1981. *Life in Moving Fluids.* Princeton University Press, Princeton. 352 pp.

Williams, T. A. 1994. Locomotion in developing *Artemia* larvae: mechanical analysis of antennal propulsors based on large-scale physical models. *Bio. Bull.* **187:** 156-163.

Wu, T. Y.-T., C. J. Brokaw, and C. Brennen. 1974. *Swimming and Flying in Nature.* Plenum Press, New York and London.

Zaret, R. E., and W. C. Kerfoot. 1980. The shape and swimming technique of *Bosmina longirostris*. *Limnol. Oceanogr.* **25:** 126–133.